Journal of The Electrochemical Society, 148 (2) G36-G42 (2001)
0013-4651/2001/148(2)/G36/7/$7.00 © The Electrochemical Society, Inc.

Crystal Surface Defects and Oxygen Gettering in Thermally Oxidized Bonded SOI Wafers

P. Papakonstantinou,[a,z] K. Somasundram,[b] X. Cao,[b] and W. A. Nevin[b]

[a]School of Electrical and Mechanical Engineering, University of Ulster, Newtownabbey, County Antrim BT37 OQB, NI, United Kingdom
[b]BCO Technologies-Analog Devices, Incorporation Belfast BT17 0LT, United Kingdom

This work investigates the role of interstitial oxygen content in the starting Czochralski bonding wafers, and the effects of buried layered implants and thermal processing on the formation of crystalline defects in the surface of bonded silicon on insulator (SOI) material. We found that unimplanted SOI material originating from Si with high oxygen levels ($>7.0 \times 10^{17}/cm^3$), were populated with heavy oxygen precipitation and related crystal defects, and were also characterized by low minority carrier lifetime values. However, a dramatic improvement was observed in the behavior of SOI with low oxygen levels ($6 \times 10^{17}/cm^3$), where the development of oxygen precipitation in the SOI layer was inhibited. Incorporation of a buried As ion implanted layer in high oxygen level SOI increased the lifetime of the material and suppressed the formation of oxygen precipitates through an oxygen gettering effect. The gettering efficiency of the buried defect layer was found to be related to the dose of the As ion implantation, the annealing temperature, and type of starting silicon material. A dose of $(1\text{-}5) \times 10^{15} cm^{-2}$ was sufficient for effective gettering.
© 2001 The Electrochemical Society. [DOI: 10.1149/1.1337608] All rights reserved.

Manuscript submitted May 3, 2000; revised manuscript received October 6, 2000.

Fusion-bonded silicon has become a proven, commercially viable silicon-on-insulator (SOI) substrate material.[1] To accelerate this market acceptance, and extend the range of possible applications, it is vital to characterize the material in order to eliminate defects associated with crystal quality. The quality of the SOI layer depends on the crystalline quality of the starting Czochralski (CZ) silicon wafers and the high-temperature processing steps used for the buried oxide (BOX) layer formation and bonding. It is well known that CZ silicon contains grown-in microdefects, which are created during ingot formation, and in addition, process-induced defects such as oxide nuclei, precipitates, and stacking faults (SF), which are formed during subsequent oxidation and device processing.[2,3] The presence of these defects in the active region of the silicon wafer can have a detrimental effect on the gate oxide integrity of metal oxide semiconductor (MOS) devices and on the performance of high density memory devices.[4-6]

Grown-in microdefects are caused by intrinsic point defects (interstitials and vacancies) and can be classified in two categories: those associated with the agglomeration of vacancies, termed laser scattering tomography defects (LSTD), D defects or crystal originated particles (COP), and those formed by clustering of interstitials.[7,8] The defect type, sizes, distribution, and concentration depend primarily on the ratio between the pulling rate (V) and thermal gradient at the solid-liquid interface of the growing crystal (G).[9,10] Depending on the V/G ratio an oxidation-induced stacking fault (OSF) ring is positioned near the edge of the wafer or disappears in the center. The region inside the OSF ring is dominated by vacancies. Transmission electron microscope (TEM) observations[11,12] have identified these as single, twin, or triple type octahedral vacancy agglomerates, with a thin oxide coating on their internal facets.

Oxygen is one of the most important impurities incorporated in the silicon, so that its behavior has been the subject of extensive study. Oxygen in CZ silicon crystal comes from the dissolution of the quartz crucible. It is transported to the crystal-melt growth interface and segregated into the crystal. Transfer of oxygen in the melt is affected substantially by melt convection. At commonly used processing temperatures, oxygen can reach supersaturation, and this therefore leads to the formation of silicon oxide precipitates, the amount and size of which depends critically on the thermal history of the crystal (*i.e.*, dwell time),[13] vacancy concentration, and interstitial oxygen concentration. Precipitates can have both beneficial and harmful effects on the device performance. If they are located in the device-active region, they act as recombination/trap centers for carriers and can reduce the mechanical strength of the silicon wafer when their concentration becomes too high. On the other hand, they have a beneficial effect in gettering undesirable metallic impurities, provided they are confined far from the silicon surface. For this reason, thermal cycles aimed at the formation of a defect-free zone (denuded zone) at the wafer surface and a bulk region with oxygen precipitates have been developed. It is common practice to deplete the wafer of precipitates by dissociation at high temperatures and to create precipitate nuclei at low temperatures. In this respect, high temperature processing steps involved in bonded wafer fabrication might cause dissolution of oxygen and related defects and favor the formation of a defect-free SOI layer.

Traditional schemes for gettering impurities in bulk silicon wafer processing include intrinsic methods such as the formation of oxygen precipitates, as described above, or extrinsic gettering involving

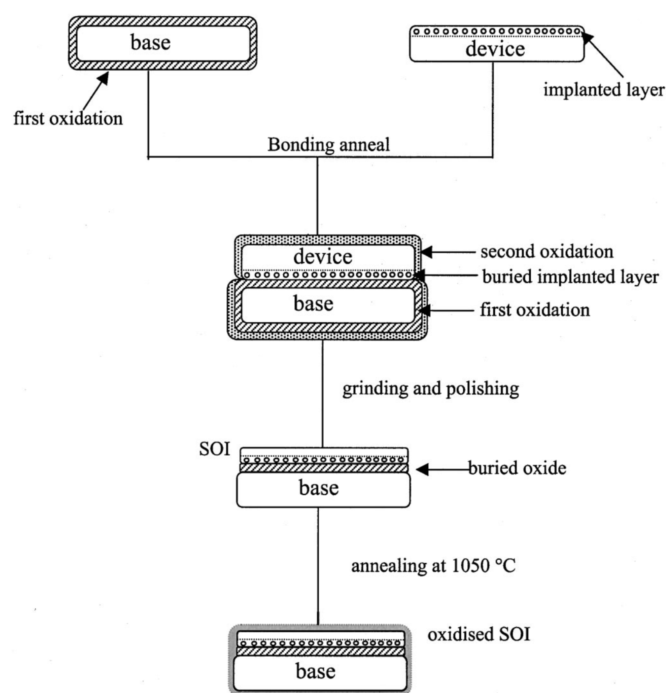

Figure 1. Schematic diagram of the bonding procedure.

[z] E-mail: P.Papakonstantinou@ulst.ac.uk

the creation of defects on the back of the wafer, for example, by mechanical damage, deposition of polysilicon, or the incorporation of high levels of dopants. However, in the case of SOI, the presence of the buried oxide tends to prevent impurities from reaching any bulk or back-side gettering sites in the handle (''base'') wafer, so that these schemes are not effective. Any viable gettering method will therefore require the formation of sites in the SOI layer. Since the intrinsic oxygen precipitate/denuded zone scheme is impractical for SOI, we have attempted to create an internal gettering sink at the bottom of the SOI layer, by fabricating a buried implanted defect layer at the bonded interface of the SOI.

There is a continuing need for noninvasive, cost effective analysis of silicon material. Carrier lifetime is an excellent predictor of defects, whether such defects are metallic contaminants or structural imperfections (*e.g.*, oxygen precipitates, SF, and dislocations, etc.).[14] These defects are potential lifetime killers; thus, the lower the defect density, the higher the lifetime. After evaluating several techniques, we chose the surface charge analyzer (SCA)[15] as a suitable commercial instrument for noncontact, nondestructive lifetime measurement. The salient feature of this measuring system is that it contains an insulating probe electrode, which when brought into contact with the oxidized silicon wafer automatically forms a capacitor structure. A collimated beam of intensity modulated light ($\lambda = 560$ nm) passes through the transparent probe electrode onto the surface of the semiconductor where it produces an induced ac photocurrent and a resulting ac-surface photovoltage (ac-SPV). The width of the surface depletion layer, W_d, and surface capacitance, C_s, are determined from the magnitude of the ac-SPV. The surface recombination lifetime τ_s is measured from the phase delay of the SPV signal. τ_s related to the surface recombination velocity, providing information on the quality of the silicon oxide interface. The sensitivity to surface and subsurface Si regions make SCA a promising tool in electrical monitoring of advanced IC processing technologies.

Although there is a great deal of knowledge about the behavior of crystalline defects in bulk silicon, very little understanding of the crystalline- and process-induced defects in bonded SOI is available. The object of this work was to study the influence of interstitial oxygen concentration and buried implant dose on the microdefect density of thermally processed SOI layers. SCA was used as an indirect way of evaluating the quality of the SOI. Moreover, the lifetime results have been correlated with the distribution of microdefects, as revealed by phase sensitive Nomarsky and atomic force microscopies after Secco etching.[16]

Experimental

Starting materials for the SOI layer were p (boron doped) and n (phosphorous doped) type (100) Czochralski (CZ) silicon ''device'' wafers of 125 mm diam, 600 μm thick, with resistivity of 3-5 Ω-cm. The oxygen concentration, as measured by Fourier transform infrared (FTIR) spectrosopy,[17] was varied between $(5.8\text{-}7.2) \times 10^{17}/\text{cm}^3$. In the following discussion, oxygen concentrations of $(5.8\text{-}6.0) \times 10^{17}/\text{cm}^3$ are deemed as low oxygen content, while oxygen concentrations equal to or higher than $7 \times 10^{17}/\text{cm}^3$ are deemed as high oxygen content. The device wafers were blanket-implanted, before bonding, with 40-80 keV As ions over a dose range of from 3×10^{13} to 5×10^{15} As ions/cm^2.

The fabrication process of the bonded SOI wafers is illustrated in Fig. 1. A base CZ or float zone (FZ) Si wafer was oxidized at 1100°C in wet O_2 before bonding to grow an oxide layer of 450 nm, which became the BOX in the SOI wafer. Bond annealing was carried out at 1050°C for 1 h in an oxygen atmosphere. Thinning of the SOI layer to 20 μm was carried out by a grinding and chemical mechanical polishing procedure.[18] Both bulk and SOI wafers were subsequently annealed at 1050°C in a dry or wet O_2 ambient to create a 100 or 500 nm thermal oxide layer. The wafers were precleaned using modified RCA1 and RCA2 baths prior to any heat-

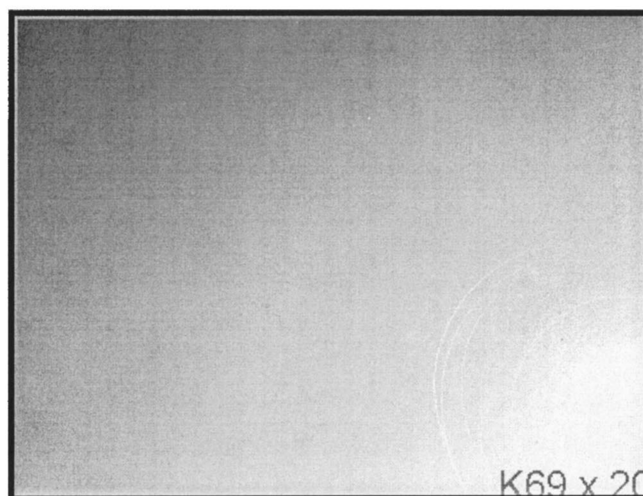

a) $6e^{17}$[Oi] / cm^3

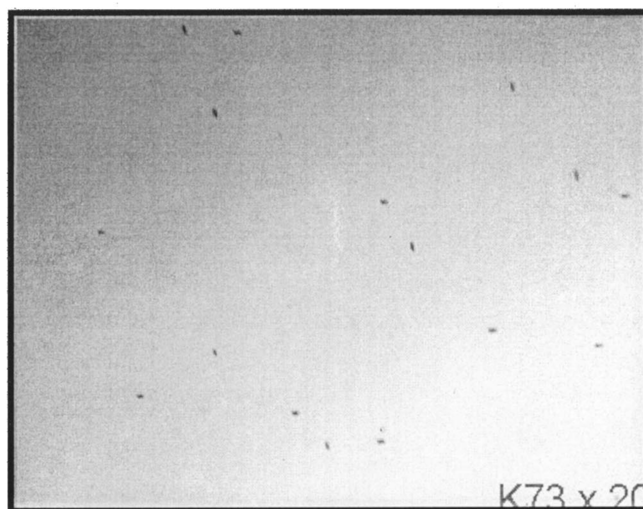

b) 6.6 e^{17}[Oi] / cm^3

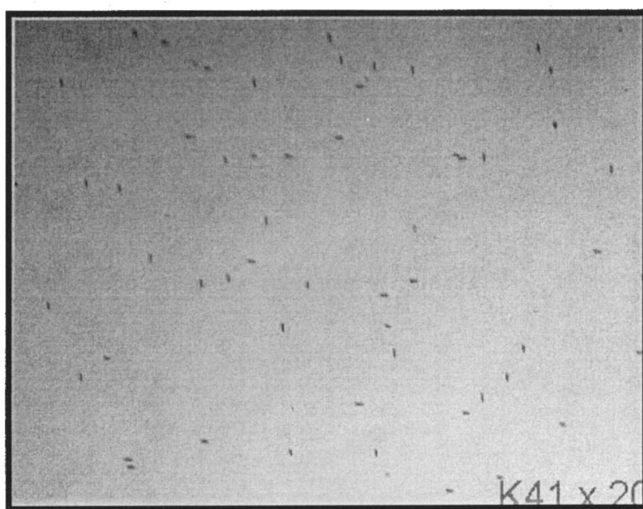

c) 7.2 e^{17}[Oi] / cm^3

Figure 2. Nomarsky images of microdefects of the p-type SOI layers with various oxygen contents after growth of a 500 nm oxide layer at 1050°C.

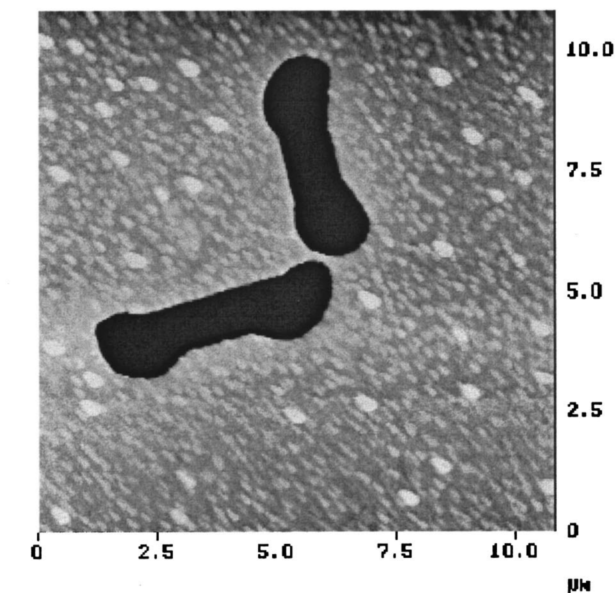

a)

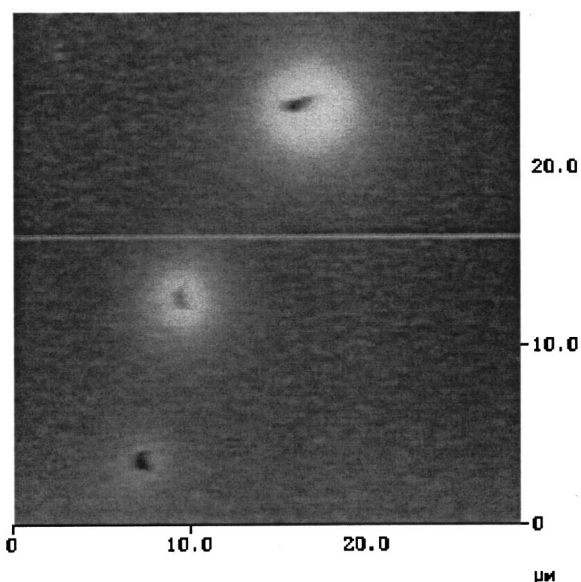

b)

Figure 3. AFM images of microdefects of the p-type SOI layers with various oxygen contents after a growth of 500 nm oxide layer at 1050°C.

treatment. The removal of metals was the main purpose of the second part of the cleaning.

Variations in the electrical and structural parameters of the thermally oxidized SOI and bulk wafers were studied by an SCA minority carrier lifetime nine-point mapping method, using a Semitest model SCA2500 instrument. The nine points were located across and along the wafer surface. The SCA signal was generated by a short 560 nm wavelength illumination that ensured shallow penetration depth (1.8 μm) of the incident light and enabled carrier lifetime measurement in the near-surface region of the SOI layer. At this penetration depth almost all carriers were photogenerated within the surface depletion layer and all minority carriers were swept by the electric field toward the surface. This made SCA measurements insensitive to diffusion effects and provided effective separation of the surface from the bulk-related effects.

Table I. Lifetime and defect density *vs*. oxygen content in p-type SOI layers after a 500 nm wet oxidation.

SOI type	Oxygen concentration ($\times 10^{17}$[O_i]/cm^3)	Average lifetime (μs)	Defect density (defects/cm^2)
p-Type CZ	6	123	1.5×10^3
p-Type CZ	6.6	98	3.2×10^4
p-Type CZ	7.2	86	5.8×10^4

After SCA analysis the wafers were stripped of the surface oxide, immersed in Secco etch solution for 1.5 min and subsequently cleaned. Examination of the etched surface by optical and atomic force microscopy (AFM) revealed the nature and distribution of crystalline imperfections present. Defect densities were estimated by counting the number of defects in several optical microcrographs of each sample. The defect density could not be determined by optical observations when the density was lower than $5 \times 10^2/cm^2$.

Results and Discussion

Characterization of bulk and SOI wafers as a function of oxygen concentration.—Figure 2 shows representative examples of Nomarsky-imaged microdefects on Secco etched p-type SOI, after growth of a 500 nm wet oxide layer at 1050°C. Optical inspection revealed two types of microdefects, oxygen precipitates and stacking faults. The microdefects in each wafer were not always distributed uniformly throughout the whole wafer. The symmetrical geometry of the patterns revealed that they were related to the crystal growth process.

Figure 3 shows the morphology of microdefects imaged by AFM. Secco etching delineates oxygen precipitates as protrusions,[19] SF as rods, and D defects or dislocations as etch pits. Stacking faults, dislocations, and D defects are areas under stress, which are etched more rapidly than normal single-crystal silicon giving rise to an engraved morphology. On the other hand, the removal rate of an oxide precipitate is lower than that of silicon and therefore protrusions are formed. Figure 3a presents a pair of SFs formed at right angles. Each SF is bounded by partial dislocations. SFs were formed by agglomeration of excess silicon self-interstitials created at the Si/SiO_2 interface during oxidation. It is interesting that in the heavily doped oxygen material the SF appeared in the central part of a protrusion (Fig. 3b), demonstrating that the oxygen precipitates act as nucleation sites for the SF formation. Dislocations were identified as etch pits whose shape varied from circular to elliptical due to the isotropic character of the etchant. The circular shape is associated with dislocations that intercept the surface at an angle of 90° while the elliptical etch pits depict dislocations intercepting the surface at less than 90°.

Average lifetimes and microdefect densities found in p-type SOI with various oxygen concentrations are summarized in Table I. Each lifetime is the average of nine point measurements taken on several wafers with exactly the same specification. It is clearly seen that the interstitial oxygen concentration, [O_i], in the bonding device wafer plays a leading role in determining the microdefect content in these bonded SOI layers. It is apparent that the defect density increases with oxygen content. Moreover, the defect density strongly correlates with the measured minority carrier lifetimes. The lower the lifetime, the higher the amount of observed defects. Almost no microdefects were observed in SOI with oxygen levels below 6×10^{17} [O_i]/cm^3. In contrast, heavily oxygen-doped bonded wafers have a highly defected surface, populated with precipitates and OSFs. The results suggest that under standard thermal conditions for device processing the oxygen concentration should be kept at low levels.

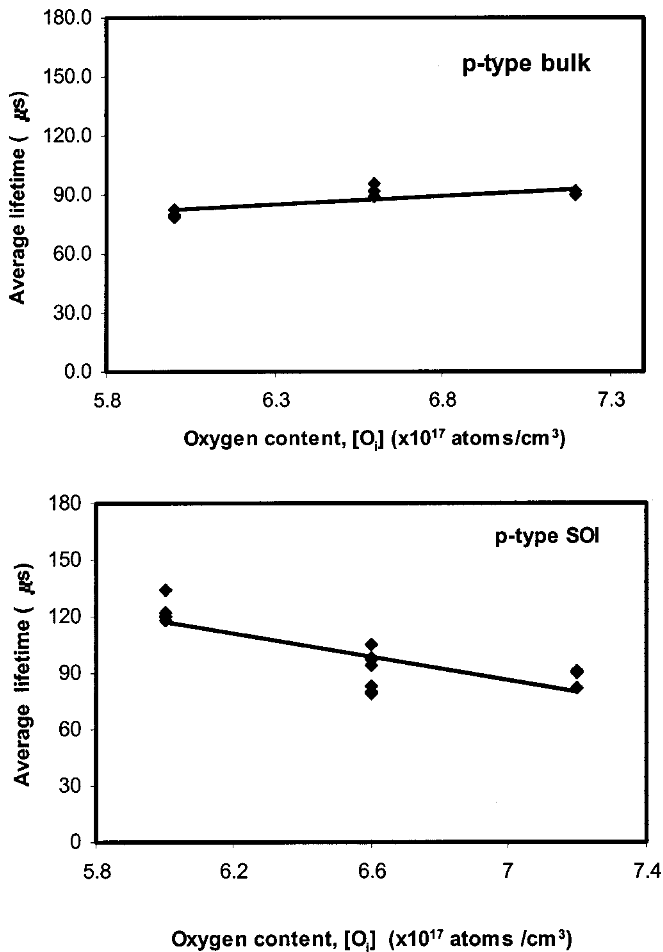

Figure 4. Average minority carrier lifetime *vs.* oxygen concentration in oxidized p-type (a, top) bulk Si wafers and (b, bottom) SOI layers.

To further demonstrate the elimination of oxidation-induced defects in low-oxygen content SOI, we carried out the same bonding and oxidation procedure using float zone (FZ) Si as the device starting material, in which the oxygen level is two orders of magnitude lower. As expected no defects could be observed, while a high minority carrier lifetime of around 200 μs was obtained.

The dependence of the average lifetime on the oxygen concentration in p-type bulk and SOI wafers is shown in Fig. 4a and b, respectively. Although no appreciable difference was observed in the lifetime of bulk wafers with various oxygen levels, the p-type SOI wafers showed a decrease in lifetime with increasing oxygen concentration. The different behavior between p-type bulk and SOI is probably due to their dissimilar annealing times. The extended high-temperature annealing encountered in the SOI wafers (which underwent two thermal treatments) was effective in demonstrating the difference between SOIs with low and high oxygen concentrations. During the second oxidation treatment the small precipitations in low $[O_i]$ SOI are dissolved out while in the high $[O_i]$ SOI are growing by gettering of oxygen atoms. Furthermore, SFs are formed in the stress field of oxygen precipitates.

Table II summarizes average lifetimes and microdefect densities found in n-type SOI with various oxygen concentrations. Again, we observe a degradation in average lifetime and an associated increase in microdefect density when the oxygen concentration is increased to 7.0×10^{17} $[O_i]/cm^3$.

Characterization of SOI as a function of oxygen concentration and As buried implant dose.—Buried layer (BL) substrates[20-22] formed by high-energy implantation are emerging as an attractive alternative to epitaxial substrates where high performance is required at lower cost. A BL is a heavily doped region that is placed beneath the active device region by ion implantation. Both the doping and damage characteristics of the BL influence the device performance. It offers benefits of latch-up prevention, diode leakage reduction, gate oxide integrity (GOI) improvement, and the possibility of proximity gettering of metallic impurities. In addition BL structures getter oxygen very effectively near the surface, preventing the formation of oxygen precipitates.[23,24]

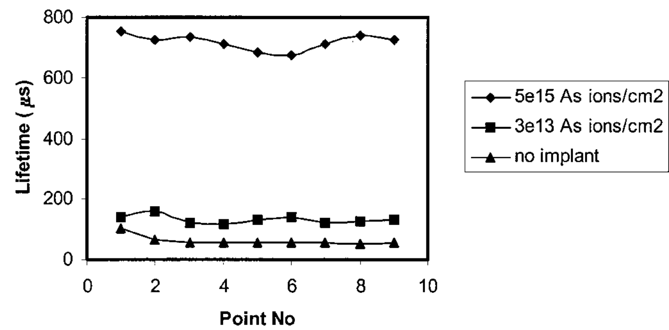

Figure 5. Minority carrier lifetime measurements on oxidized n-type SOI wafers implanted with various As ion doses.

In order to investigate the gettering effects of buried low-energy As implanted SOI layers we conducted the following experiments. Active device wafers, having a range of oxygen contents, were implanted with 40-80 keV As ions at doses of between 3×10^{13} and 5×10^{15} As ions/cm^2. Following implantation the device wafers were bonded, thinned, and subsequently annealed at 1050°C in a wet O_2 ambient for 1 h. The thermally oxidized SOI wafers were then evaluated for OSFs and changes in minority carrier lifetime.

Figure 5 shows the effect of the As implant dose on lifetime in bonded SOI n-type layers with a high oxygen content, measured at nine points over the wafer surface. The lifetime is seen to increase dramatically from ~50 μs for unimplanted samples to ~720 μs at the highest implant dose. The appreciable increase in lifetime of the heavily implanted SOI is evidence that damage extending throughout a buried implanted region toward the surface can act as a gettering sink for oxygen. In addition to oxygen this work does not rule out the possibility of gettering metallic impurities, thus reducing their concentration in the active device region.

It is now widely accepted[25,26] that when dopant ions are implanted into a silicon target, many interstitial-vacancy (Frenkel) pairs and an amorphous layer are generated by collisions between the energetic ions and silicon atoms, around the projected range, R_p, of the ions. During the first bond annealing treatment, the amorphized layer is recrystallized by solid phase epitaxy, and the majority of point defects agglomerate to form vacancy clusters and interstitial dislocations around R_p. The remainder of these, and particularly those beyond R_p, remain free and diffuse to regions of lower defect concentration in the bulk and towards the SOI wafer surface, where they may cluster and become oxygen-precipitate nuclei. The nucleation processes are aided by the vacancy-oxygen in-

Table II. Lifetime and defect density *vs.* oxygen content in n-type SOI layers after a 500 nm wet oxidation.

SOI type	Oxygen concentration ($\times 10^{17}$ atoms/cm^3)	Average lifetime (μs)	Defect density (defects/cm^2)
n-Type CZ	5.9	133	2.8×10^3
n-Type CZ	6.4	138	1.1×10^3
n-Type CZ	6.7	150	4.9×10^3
n-Type CZ	7.0	102	9.2×10^4

Table III. Lifetime and defect density in n-type SOI for various oxygen contents and arsenic implant doses, after a 500 nm wet oxidation.

SOI type	Oxygen concentration ($\times 10^{17}$ atom/cm^3)	As implant dose (atom/cm^2)	Average lifetime (μs)	Defect density (defects/cm^2)
n-Type CZ	6.0	0	71	8.0×10^3
n-Type CZ	7.0	0	54	9.1×10^4
n-Type CZ	5.9	3×10^{13}	169	5.1×10^3
n-Type CZ	7.0	3×10^{13}	131	1.4×10^5
n-Type CZ	5.9	5×10^{15}	605	2.2×10^3
n-Type CZ	7.0	5×10^{15}	717	1.5×10^3

teractions and the dislocation strain fields. We consider the vacancy-interstitial defects formed at and beyond the projected range R_p to be one of the mechanisms responsible for the gettering of oxygen atoms.

Results of minority carrier lifetime measurements and defect densities for n-type SOI as functions of oxygen concentration and As buried implant dose are summarized in Table III. The reason for the different values for unimplanted wafers between Tables II and III is because the wafers were taken from different ingots, and oxidized in different furnace runs. However, we observe the same basic trends in both sets of samples, *i.e.*, unimplanted low oxygen content SOI layers have a low density of precipitate-type defects, while the unimplanted high oxygen content SOI have a much higher density of defects and a lower minority carrier lifetime. Similar tendencies are also seen with the 3×10^{13} As ions/cm^2 samples, indicating that at this low dose the defected As buried layer has little gettering ability. In fact, the high oxygen samples showed higher defect density and a greater proportion of OSFs compared to the unimplanted samples. However, a significant improvement was observed for the samples implanted with the highest dose studied, 5×10^{15} As ions/cm^2. In addition to an increase in the minority carrier lifetime by approximately an order of magnitude, we were able to produce SOI using high-oxygen material, which was almost free of defects, *i.e.*, gettering is effective only at high implant dose. This can be seen clearly in the optical micrographs of Fig. 6, which compares the defect density for high oxygen samples with different implant doses. To unambiguously identify the gettering of oxygen, further investigations in this area, using techniques such as secondary ion mass spectroscopy (SIMS) and cross-sectional transmission electron microscopy (TEM), will be necessary.

For SOI prepared using FZ device material, the gettering effect of the implant was clearly seen by measured minority lifetimes of around 800 μs, compared to 200 μs for unimplanted material. Again, no defects were observed in the SOI layers of these samples.

The defect densities for p-type SOI as functions of oxygen concentration and As buried implant dose are summarized in Table IV. In this case, it was found that an implant dose of 1×10^{15} As ions/cm^2 was sufficient to getter the oxygen and reduce the density of OSFs. However, in this case, a further increase of implant dose to 5×10^{15} appeared to reduce the gettering efficiency. Interestingly, as with the n-type material, the highest density of defects was observed with the combination of high-oxygen material and low-dose implantation.

Comparing the results obtained for the n- and p-type material examined in this study, while the overall trends are similar, subtle differences are observed between the two types of material. In particular, OSF defect generation appears to be facilitated at lower oxygen levels in p-type SOI, while the optimum buried implant dose needed to suppress defect formation is lower in the p-type material. These effects may be related to differences in the properties of the raw material silicon formed during the crystal growth process, such as the distribution and concentration of grown-in defects and nucleation site precursors.

Table IV. Defect density in p-type SOI for various oxygen contents and arsenic implant doses, after a 500 nm wet oxidation.

SOI type	Oxygen concentration ($\times 10^{17}$atom/cm^3)	As implant dose (atom/cm^2)	Defect density (defect/cm^2)
p-Type CZ	6.0	0	7.0×10^2
p-Type CZ	7.2	0	3.8×10^4
p-Type CZ	6.0	3×10^{13}	7.3×10^2
p-Type CZ	7.2	3×10^{13}	2.6×10^5
p-Type CZ	6.0	1×10^{15}	3.7×10^3
p-Type CZ	7.2	1×10^{15}	4.2×10^3
p-Type CZ	6.0	5×10^{15}	5.5×10^2
p-Type CZ	7.2	5×10^{15}	3.4×10^4

Table V. Lifetime and defect density in n-type CZ SOI processed with or without a prebond low-temperature oxygen precipitate nucleation cycle.

Precipitation cycle	As implant dose (atom/cm^2)	Average lifetime (μs)	Defect density (defect/cm^2)
Without	0	130	2×10^3
With	0	110	8×10^4
Without	5×10^{15}	560	$<1 \times 10^3$
With	5×10^{15}	420	9×10^4

Effect of oxygen precipitate nucleation on defect generation in SOI.—In order to effectively form oxygen precipitates, regardless of the oxygen concentration of the starting SOI, we deliberately subjected unimplanted and implanted n-type SOI device wafers to a standard low-temperature oxygen precipitate nucleation anneal at 700°C preceding the high-temperature bond annealing. After bonding and thinning, a dry oxide layer of 100 nm was grown at 1050°C on top of the SOI. Table V compares the results for SOI prepared with or without the thermal precipitation cycle. Defect densities are an order of magnitude higher and the lifetimes are lower, for the low-temperature processed SOI. It is well established that low-temperature thermal treatment of silicon is a precipitate nucleation step in which many tiny nuclei are generated and practically no precipitate growth occurs.[27] Then, in a subsequent high-temperature treatment, such as that used here for the bond-annealing step, the small nucleation sites grow by capturing diffusing oxygen. In the case, with the high level of nucleation, the gettering effect of the implant is insufficient to limit the growth of precipitates, and no reduction in defect density is observed compared to unimplanted samples. The results therefore indicate that the postimplant processing must carefully avoid low temperature treatments.

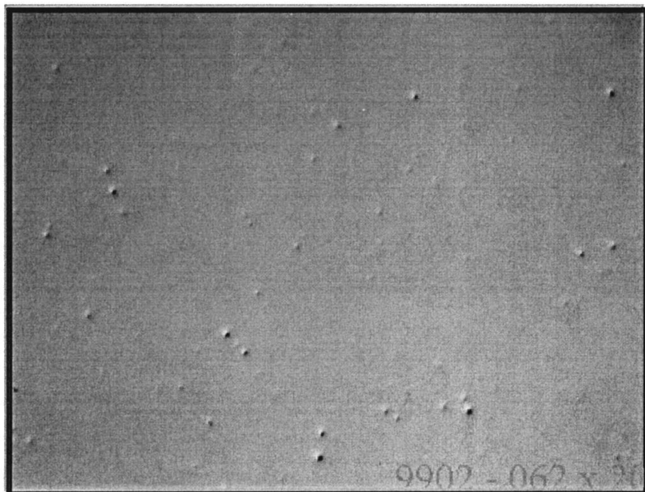

a) No implant

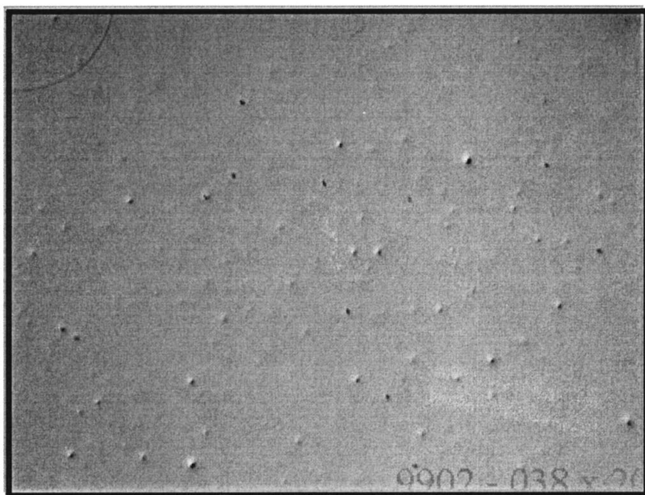

b) $3e^{13}$ As^+/cm^2

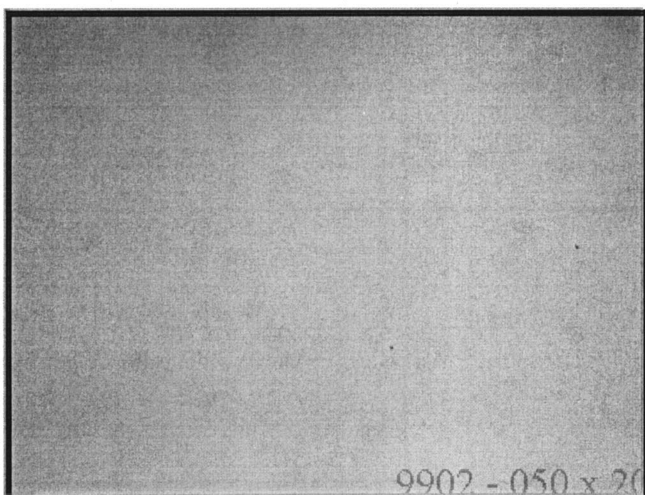

c) $5e^{15}$ As^+/cm^2

Figure 6. Nomarsky images of microdefects of n-type, thermally processed SOI layers with oxygen content of 7×10^{17} atom/cm^3 implanted with various As ion doses.

Conclusions

We have investigated the role of interstitial oxygen content in the starting CZ bonding device wafers, and the effects of buried layered implants and thermal processing on the formation of crystalline defects in the surface of bonded SOI material. The SCA was used to measure the carrier recombination lifetime of both implanted and unimplanted bonded SOI after high-temperature oxygen treatment, while Secco etching in conjunction with optical and atomic force microscopies has been used to assess the defect type and concentration. Defect-free SOI layers have been realized using low oxygen content starting material and by avoiding the use of low-temperature thermal processing. SOI layers originating from heavily doped oxygen Si ($>7.0e^{17}/cm^3$), were populated with heavy oxygen precipitation and related crystal defects, and characterized by low minority carrier lifetime values. Furthermore, wafers processed through deliberate oxygen precipitation cycles prior to bonding gave very low lifetimes and high levels of defects, as revealed by Secco etching. Oxygen gettering in heavily oxygen-doped SOI was implemented by introducing crystalline defects in the base of the SOI, by means of an As implantation process, prior to wafer bonding. As a result significant improvements in the lifetime and microdefect density were achieved. While the overall trends, between the n-type and p-type materials used in this study were similar, subtle differences were observed in the defect generation behavior and the optimum implant gettering dose.

Acknowledgments

The authors thank Dieter Gräf and Norbert Hinterschwepfinger of Wacker Siltronic AG for the oxygen content measurements and useful discussions, as well as Kevin Yallup and Scott Blackstone for their many helpful suggestions.

BCO-Technologies-Analog Devices assisted in meeting the publication costs of this article.

References

1. Q.-Y. Tong and U. Gösele, *Semiconductor Wafer Bonding: Science and Technology*, Wiley, New York (1999).
2. K. M. Kim, *Solid State Technol.,* **39**, 70 (1996).
3. K. M. Kim, *Solid State Technol.,* **43**, 69 (2000).
4. B. O. Kolbesen and H. Cerva, in *Defects in Silicon*, T. Abe, W. M. Bullis, S. Kobayashi, W. Lin, and P. Wagner, Editors, PV 99-1, p. 19, The Electrochemical Society Proceedings Series, Pennington, NJ (1999).
5. G. Park, J. M. Park, K. C. Cho, G. S. Lee, and H. K. Chung, in *Crystalline Defects and Contamination*, B. O. Kolbesen, P. Stallhofer, C. Claeys, and F. Tardiff, Editors, PV 97-22, p. 173, The Electrochemical Society Proceedings Series, Pennington, NJ (1997).
6. G. Rozgonyi, M. Tamatsuka, K. M. Bae, and F. Gonzalez, in *Crystalline Defects and Contamination*, B. O. Kolbesen, P. Stallhofer, C. Claeys, and F. Tardiff, Editors, PV 97-22, p. 153, The Electrochemical Society Proceedings Series, Pennington, NJ (1997).
7. H. Yamagishi, I. Fesegawa, N. Fujimaki, and M. Katayama, *Semicond. Sci. Technol.,* **7**, A135 (1992).
8. D. Graf, M. Suhren, U. Lambert, R. Schmolke, A. Ehlert, W. Von Ammon, and P. Wanger, *J. Electrochem. Soc.,* **145**, 275 (1998).
9. V. Voronkov, R. Falster, and J. C. Holzer, in *Crystalline Defects and Contamination*, B. O. Kolbesen, P. Stallhofer, C. Claeys, and F. Tardiff, Editors, PV 97-22, p. 3, The Electrochemical Society Proceedings Series, Pennington, NJ (1997).
10. T. Sinno, R. A. Brown, W. von Ammon, and E. Dornberger, *J. Electrochem. Soc.,* **145**, 302 (1998).
11. M. Kato, T. Yoshida, Y. Ikeda, and Y. Kitagawara, *Jpn. J. Appl. Phys., Part 1,* **35**, 5597 (1996).
12. T. Ueki, M. Itsumi, and T. Takeda, *Jpn. J. Appl. Phys., Part 1,* **36**, 1781 (1997).
13. S. S. Kim and W. Wijaranakula, *J. Electrochem. Soc.,* **142**, 553 (1995).
14. D. K. Schroder, *IEEE Circuits Devices Mag.,* **14**, 14 (1998).
15. E. Kamieniecki, in *Analytical and Diagnostic Techniques for Semiconductor Materials*, B. O. Kolbesen, C. Claeys, P. Stallhofer, F. Tardif, J. Benton, T. Shaffner, D. Schroder, S. Kishino, and P. Rai Choudhury, Editors, PV 99-16, p. 259, The Electrochemical Society Proceedings Series, Pennington, NJ (1999).
16. F. Secco d' Aragina, *J. Electrochem. Soc.,* **119**, 948 (1972).
17. K. Krishnan, *Biorad Semicond. Notes,* **102**, (1983).
18. S. Blackstone, in *Semiconductor Wafer Bonding: Physics and Applications III*, C. E. Hunt, H. Baumgart, S. S. Iyer, T. Abe, and U. Gösele, Editors, PV 95-7, p. 56, The Electrochemical Society Proceedings Series, Pennington, NJ (1995).
19. A. C. Benkitsch, J. Lutz, and F. Kuchar, *Inst. Phys. Conf. Ser.,* **160**, 17 (1997).
20. H. Wong, N. W. Cheung, P. K. Chu, J. Liu, and J. W. Mayer, *Appl. Phys. Lett.,* **52**, 1023 (1988).
21. T. Kuroi, Y. Kawasaki, S. Komori, K. Fukumoto, M. Inuishi, K. Tsukamoto, H.

Shinyashiki, and T. Shingyoji, *Jpn. J. Appl. Phys.,* **32**, 303 (1993).
22. L. Rubin, *Solid State Technol.,* **42**, 95 (1999).
23. A. Agarwal, K. Christensen, D. Venables, D. M. Maher, and G. A. Rozgonyi, *Appl. Phys. Lett.,* **69**, 3899 (1996).
24. R. Job, W. R. Fahrner, A. G. Ulyashin, Y. A. Bumay, A. I. Ivanov, and L. Palmetshofer, *Solid State Phenom.,* **57-58**, 91 (1997).
25. M. D. Giles, S. F. Yu, H. W. Kennel, and P. A. Packan, *Solid State Technol.,* **41**, 97 (1998).
26. Y. M. Gueorguiev, R. Kogler, A. Peeva, D. Panknin, A. Mucklich, R. A. Yankov, and W. Skorupa, *Appl. Phys. Lett.,* **75**, 3467 (1999).
27. Y. Shimanuki, H. Furuya, I. Suzuki, and K. Murai, *Jpn. J. Appl. Phys., Part 1,* **24**, 1594 (1985).